ACADEMIA ROMÂNĂ
Revue Roumaine de Chimie
http://web.icf.ro/rrch/

Rev. Roum. Chim.,
2020, *65*(10), 943-953
DOI: 10.33224/rrch.2020.65.10.09

PREPARATION AND CARACTERISATION OF MONTMORILLONITE-Fe^{3+} (MMT-Fe^{3+}) NANOCLAY MINERAL FOR CRYSTAL VIOLET (CV) REMOVAL FROM AQUEOUS SOLUTIONS

Soufiane BOUDJEMAA[a,b,*]

[a] Laboratory of Chemical Process Engineering, Ferhat Abbas setif 1 University, Algeria
[b] Faculty of Sciences and Technology, Mohamed El Bachir El Ibrahimi B.B.A University, Algeria

Received August 22, 2020

Montmorillonite-Fe^{3+} (MMT-Fe^{3+}) nanoclay mineral was successfully prepared using a ferric chloride precursor. The prepared sample was characterized using IR, XRD, BET and SEM-EDX. We have explored the highly efficient and environmentally benign MMT-Fe^{3+} for adsorption of Crystal Violet (CV) dye from aqueous solution under ambient conditions. The MMT-Fe^{3+} was interacted with CV dye solution at different pH, temperature and solid-to-liquid ratio. The concentration of CV dye removal was estimated from its optical density at λ_{max} = 590 nm using UV–Vis spectrophotometer. The CV dye removal was rapid at basic pH and increases with temperature up to 40 °C. A complete reduction (100%) was occurred in about 7 min at pH 7 and 10 while at pH 3 in about 10 min. The time taken for complete reduction at 0, 30 and 40 °C are 10, 7 and 5 min respectively. The removal followed by adsorption of dye molecules on the spent nanoclay mineral was evident from SEM/EDX analysis. More importantly, MMT-Fe^{3+} could be separated and retrieved easily after the reaction by centrifugation from the degraded CV dye solution. The experimental results of CV dye removal from MMT-Fe^{3+} follows the pseudo first order kinetics. This study reveals that MMT-Fe^{3+} has the potential to be used as reductant/adsorbant to remove cationic pollutants effectively and rapidly from drinking water and large scale of industrial wastewater.

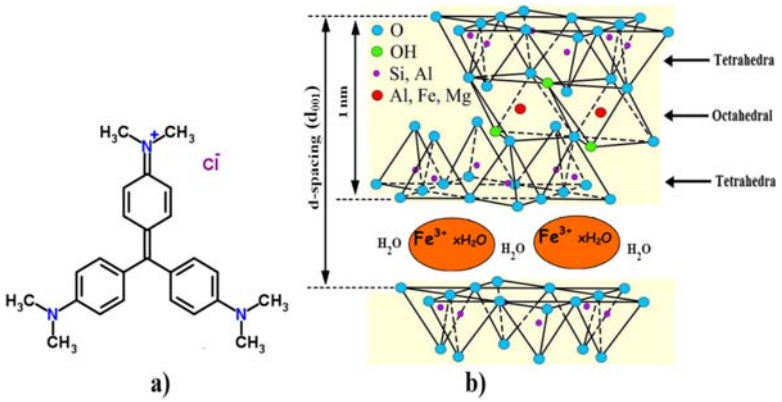

INTRODUCTION*

The contamination of water by pollutants of various origins is an actual problem.[1] In the textile industries, wastewater is one of the most important sources of pollution of surface waters and groundwater, especially for agricultural land and wildlife.[2,3] The waste products of the textile industries are enormous nuisances for human health and the environment. In fact, the various dyes used cause serious problems because of their stability and low biodegradability.[4,5]

As a starting point, Crystal Violet (CV) is a water-soluble cationic dye belonging to the class of triarylmethane dyes whose molecular structure as shown in Fig. 1a. they are widely used in textile industries for dyeing cotton, acrylic, nylon, wool, leather, paper, plastics and silk.[6] Further, it's a carcinogenic that has been classified among the recalcitrant molecules since it is poorly metabolized by microbial flora; it is not only biodegradable but it might persist in environmental medium as well.[7,8] Hence, worldwide environmental scientists have faced this threat by

* Corresponding author: bsouf77@yahoo.fr

developing cost effective and efficient technologies for CV treatment.[9]

Therefore, evolving a sustainable competitive method for effluent management for the dyeing industry has been a crucial task while targeting the environment protection.[10] Conventional physic-chemical processes for dye removal from wastewater include oxidation, photochemical degradation, reverse osmosis, membrane separation, coagulation and adsorption.[11-14] The latter is one of the most effective methods that has been successfully adopted for the removal of wastewater color.[15]

The activated carbon is a largely used adsorbent seeing that it has a high adsorption capacity of organic materials.[16] However, this adsorbent is very expensive and remains difficult to regenerate. The investigation of other effective and less expensive adsorbents demonstrated peat soil capability, clay minerals, chitin-chitosan and hydroxyapatite.[17, 18]

Clays are important class of materials that are readily available in nature. These are used as very good adsorbents, decolouration agents, ion exchangers, molecular sieves, catalysts.[19]

More importantly, clay minerals have attracted significant attention for diversified applications including pollutants removal/remediation, because of their high specific surface area, adsorption capacity and excellent adsorption behavior towards cationic sensitizers.[20]

The most used clays as nano-adsorbents are montmorillonite/ smectite group and kaolinite clays.[21] Cu(II) exchanged montmorillonite[22] and TiO_2 pillared montmorillonites[23] are successfully employed for the adsorption and degradation of dyes.

Montmorillonite (MMT) is a 2:1 smectite group clay mineral, comprises of one octahedral sheet of Al^{3+} grid sandwiched between two tetrahedral sheets of Si^{4+} having required qualities such as low diffusion, high absorption capacity, low hydraulic conductivity and layered structure.[24] The permanent negative charge of montmorrllonite is attributed to the isomorphous replacement of Al^{3+} for Si^{4+} in the tetrahedral layer and Mg^{2+} for Al^{3+} in the octahedral layer.[25] Such a permanent negative layer charge is balanced by exchangeable cations like Ca^{2+}, Na^{+} etc. at the interlayer. *i.e.*, the redox sensitive Fe^{3+} ions are placed in the interlayer of MMT becomes MMT- Fe^{3+} as shown in Fig. 1b.[26] Thus, the cation exchange capacity (CEC) of clay mineral depends on the net elemental composition that varies with the geographical availability in the environment.[27] The properties and uses of this clay mineral can be modified not only by altering the structural Fe^{2+}/ Fe^{3+} ratio[28], but also by replacing the interlayer cations with a variety of inorganic and organic cations.[29] Environmentally benign and redox sensitive metal ions like ferrous and ferric ions in the interlayer of smectite clay mineral can impart many technological important properties. It is obvious that the development of new method which involves heterogeneous reaction would be suitable for large-scale synthesis.[30] Fe-pillared montmorillonite or Fe^{3+} incorporated clay minerals has been extensively used in heterogeneous catalytic systems and were proved to be advantageous in both economic and environmental point of view.[31]

The availability as well as the amount or access of Fe^{3+} ions for dye degradation was very limited. Hence it is important to make use of MMT-Fe^{3+}, *i.e.*, the redox sensitive Fe^{3+} ions are placed in the interlayer of clay mineral to augment the real field applications.[32] Recently, Jlassi *et al*.[33] has reported the preparation of MMT-Fe^{3+} and explained the basic properties along with stability. Hence, it is possible to make use of such an important redox sensitive clay mineral for the adsorption of dye.

The main objective of the present study is the application of MMT-Fe^{3+} as an effective reductant for CV dye removal in aqueous solution. The reduction reaction was carried out at different pH and temperature by varying the amount of MMT-Fe^{3+}. However, to till date, the use of Fe nanoclay minerals as a reductant/adsorbent for the adsorption of dyes was limited. Hence facile and reliable preparation of MMT-Fe^{3+} nanoclay mineral is having excellent adsorption and degradation properties make a suitable reductant for removal of CV dye from aqueous solution.

EXPERIMENTAL

1. Materials

Natural montmorillonite (MMT) was supplied by the County of Maghnia, Western Algeria, and used after purification. The structural formula of raw montmorillonite nanoclay mineral is given as $Na_{0.35}K_{0.01}Ca_{0.02}(Si_{3.89}Al_{0.11})(Al_{1.60}Mg_{0.32}Fe_{0.08})O_{10}(OH)_2\ nH_2O$ with a cation exchange capacity (CEC) of about 95 meq/g. The chemical composition of MMT is given in Table 1.

The pure MMT was modified through cation exchange with a NaCl (1M) aqueous solution to obtain sodium montmorillonite (MMT-Na).[34]

The pollutant used in this study is a Crystal Violet (CV) {Tris(4-(dimethylamino)phenyl)methylium chloride}, was obtained from Sigma–Aldrich and was used without further purification. The dye has molecular formula $C_{25}N_3H_{30}Cl$ and molecular weight 407,98 g/mol. The structure of this dye is shown in Fig. 1a. The ferric chloride ($FeCl_3$) and silver nitrate ($AgNO_3$) were obtained from Merck, Germany.

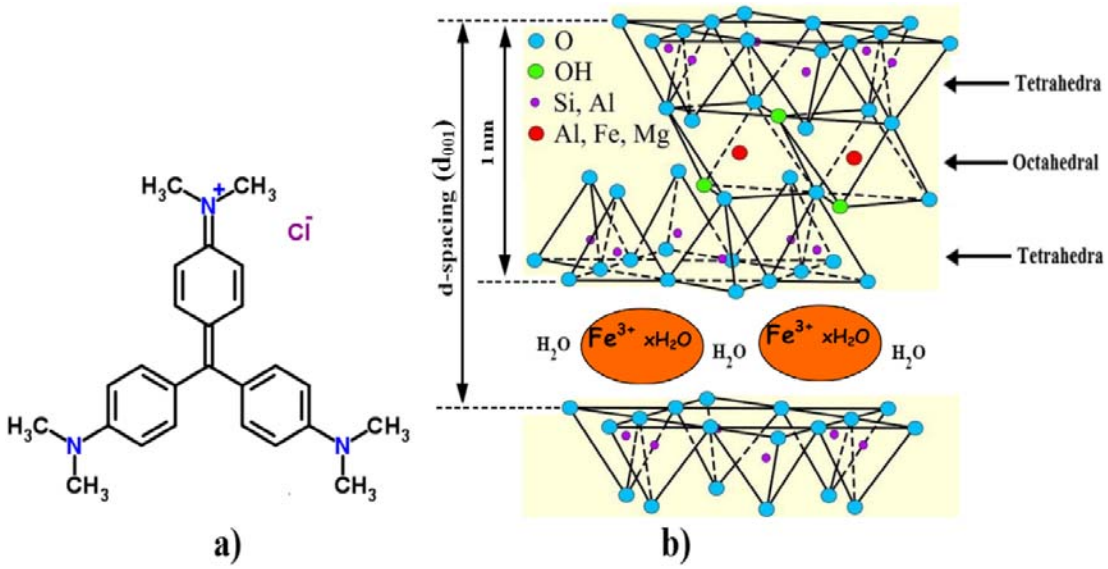

Fig. 1 – a) Molecular structure of CV dye, b) Schematic representation of MMT-Fe^{3+}.

Table 1

Chemical composition (wt %) of initial MMT according to XRF analysis

Others	SiO_2	Al_2O_3	Fe_2O_3	TiO_2	P_2O_5	SO_3	K_2O	MnO	ZrO_2	CaO
Balance	71.60	12.75	10.77	1.66	0.70	0.09	0.09	0.02	0.04	0.31

2. Preparation of MMT-Fe^{3+}

10 g of MMT-Na was added to 1 L of 0.4 M $FeCl_3$ solution and the suspension (pH = 2) so obtained was stirred for 24 h to convert the clay into MMT-Fe^{3+}. After allowing the clay mineral to settle, the supernatant solution was decanted and fresh $FeCl_3$ solution was added. After three cycles of above treatment, the clay mineral was washed with de-ionised water followed by filtration through 0.2 μm membrane filter until no chloride was detected in washing by $AgNO_3$ test. The sample was vacuum dried at room temperature and ground to fine powder for further characterization and use.

In order to estimate the interlayer iron, MMT-Fe^{3+} was subjected for cation exchange with 0.05 M H_2SO_4 for about 24 h. The ratio of ferrous to ferric ions (Fe^{2+}/Fe total where Fe_{total} = Fe^{2+} + Fe^{3+}) released was determined by 1,10 phenanthroline method[35] using UV–Vis spectrophotometer (λmax = 510 nm).

3. Crystal violet removal studies

In a typical stoichiometric case, freshly prepared MMT-Fe^{3+} (0.03 g) was added to CV dye solution (0.025 mM, 100 mL) and stirred magnetically. The reaction was also carried out at different solid-to-liquid ratio, pH 3–10 (adjusted with dil. HCl and NaOH) and temperature 0, 30 and 40 °C. The reaction mixture was withdrawn periodically by using a syringe tube and then centrifuges to separate the suspended clay particles. The decrease in the dye concentration was estimated from its optical density. The decrease in the dye concentration due to reaction between MMT-Fe^{3+} and CV dye was expressed in terms of % reduction as a function of time. The spent MMT-Fe^{3+} was separated by centrifugation, washed thoroughly with water and vacuum dried at room temperature for further characterization using X-ray diffraction (XRD), Fourier transform infrared spectroscopy (FT-IR) and field emission scanning electron microscope (SEM) with energy dispersive X-ray analysis (EDXA) techniques.

4. Characterization

X-ray diffraction (XRD) measurements were carried out Philips diffractometer (PW-1710).

Using a CuKα (λ = 1.54 Å) radiation source accelerated at 40KV and 30 mA at room temperature. All scans were performed in 2θ range 2–40 degrees with scan speed: 2 deg/min.

Fourier transform infrared spectra (FTIR) were carried out on Fourier Spectrophotometer type Shimadzu FTIR-8300 in the range of 400-4000 cm-1, using KBr disc method.

The micrographs of freshly prepared and spent MMT-Fe^{3+} was recorded using field emission scanning electron microscope (Nova Nano-SEM 600, FEI Company, Netherlands) along with energy dispersive X-ray (EDX) analysis for approximate elemental composition.

Thermal analysis was carried out in a SHIMATZU D6000 coupled to a DC ampler and temperature controller. Data from DTA-TG were obtained in all cases at a heating rate of 5°C/min between 30°C and 1000°C and under N_2 atmosphere.

The percentage of dye removal from aqueous solution was estimated from its optical density at λmax = 590 nm using UV–Vis spectrophotometer 160 A Shimadzu.

RESULTS AND DISCUSSION

1. Characterization of MMT-Fe^{3+}

The concentration of iron has been obtained from 0.5 g of MMT-Fe^{3+} using different reagents (100 mL) viz., 0.05 M H_2SO_4, 0.5 M $(NH)_4C_2O_4$, 1 M NaCl, 0.05 M Na_2EDTA. The total Fe^{3+} ions extracted was about 1.14 meq/g. In addition, XRD,

FT-IR and Field emission SEM with EDXA results confirmed the formation of MMT-Fe^{3+}.

XRD patterns of MMT-Fe^{3+}, MMT-Ca (typical divalent cation exchanged clay mineral) and MMT-Na at relative humidity RH 40% are compared (Fig. 2). The basal spacing (d_{001}) of MMT-Fe^{3+} is 15.2 Å and MMT-Ca is 14.8 Å and hence are found to be almost same, whereas d_{001} of MMT-Na is 12.2 Å. It is clear that the divalent cation exchanged clay minerals showed higher d_{001} value due to larger layer of hydration when compared to monovalent cation exchanged clay mineral. These values are in good agreement with the previously reported values.[36,37] In spent MMT-Fe^{3+}, basal spacing d_{001} value was almost same due to small amount of CV dye adsorbed on the surface area and hence it didn't show a significant peak using XRD analysis.

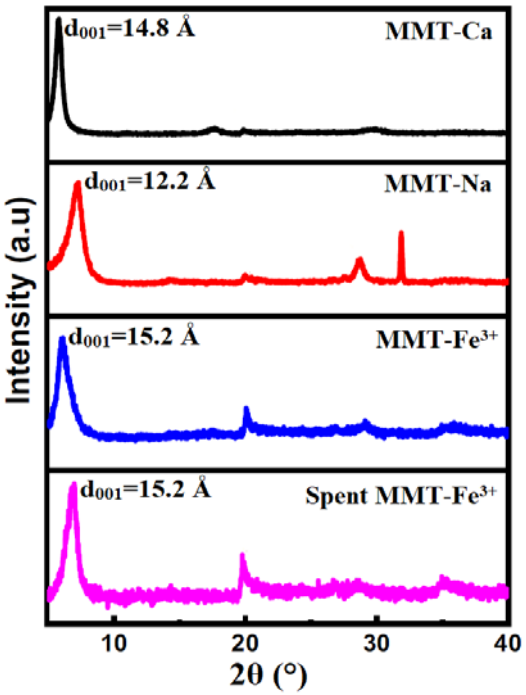

Fig. 2 – Powder XRD patterns of: MMT-Fe^{3+}, MMT-Ca, MMT-Na and spent MMT-Fe^{3+}.

As shown in Figure 3, the Fourier transform infrared (FT-IR) spectra of freshly prepared MMT-Fe^{3+} is similar to that of MMT-Na. The basic structure of clay mineral has not undergone any significant changes. For instance, the bending vibration bands at 520 cm^{-1} for Si–O–Al, and 920 cm^{-1} for Al_2OH are intact. However stretching vibrations of Si–O group at 1046 cm^{-1} are slightly broadened. The vibration bands at 1628 cm^{-1} corresponds to adsorbed water and 3429 cm^{-1} for water present at the interlayer. As revealed by Fourier transform infrared (FT-IR) spectra the spent clay mineral is intact in all respects when compared with pure MMT-Fe^{3+}.

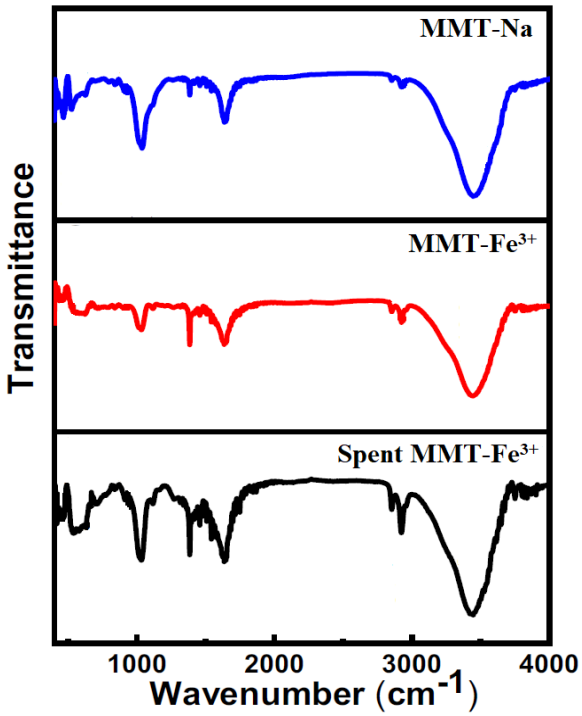

Fig. 3 – FT-IR spectra of : MMT-Fe^{3+}, MMT-Na and spent MMT-Fe^{3+}.

The thermal curves are depicted in Fig. 4 and Fig. 5 in the 30˚C – 1000 °C range. The curves correspond to the starting MMT-Na and MMT-Fe^{3+}, after equilibrating in a desiccator, at room temperature. The general feature of thermal curves clearly reveals two steps: 1) in the 30˚C – 340˚C and 2) in the 300˚C - 650˚C temperature ranges. The first step with MMT-Na and MMT-Fe^{3+} has been ascribed to physisorption of the hydrating water, whereas the second step is due to dehydroxylation of silicate structure. Sometimes, this step occurs dissociated into two which is not well visible here but is clearly shown in the corresponding TGA curve (Fig. 4), denoting dehydroxylation of the silicate structure in two different environments. For MMT-Fe^{3+}, the net isomorphic substitution in the clay with different bonding strengths between the oligocations and the surrounding oxygen (or hydroxyl) ions can be observed.[38]

Dehydroxylation continues between 337°C and 650°C and is also detected to approximately 620°C in an important step. This step is related with the stability of the MMT-Fe^{3+}, since an important decrease in the basal spacing values occurs at this

temperature, indicating the collapse of the clay structure. Therefore, the thermogravimetric analyses are in agreement with the aforementioned thermal stability of the MMT-Fe^{3+} clay up to 650˚C.

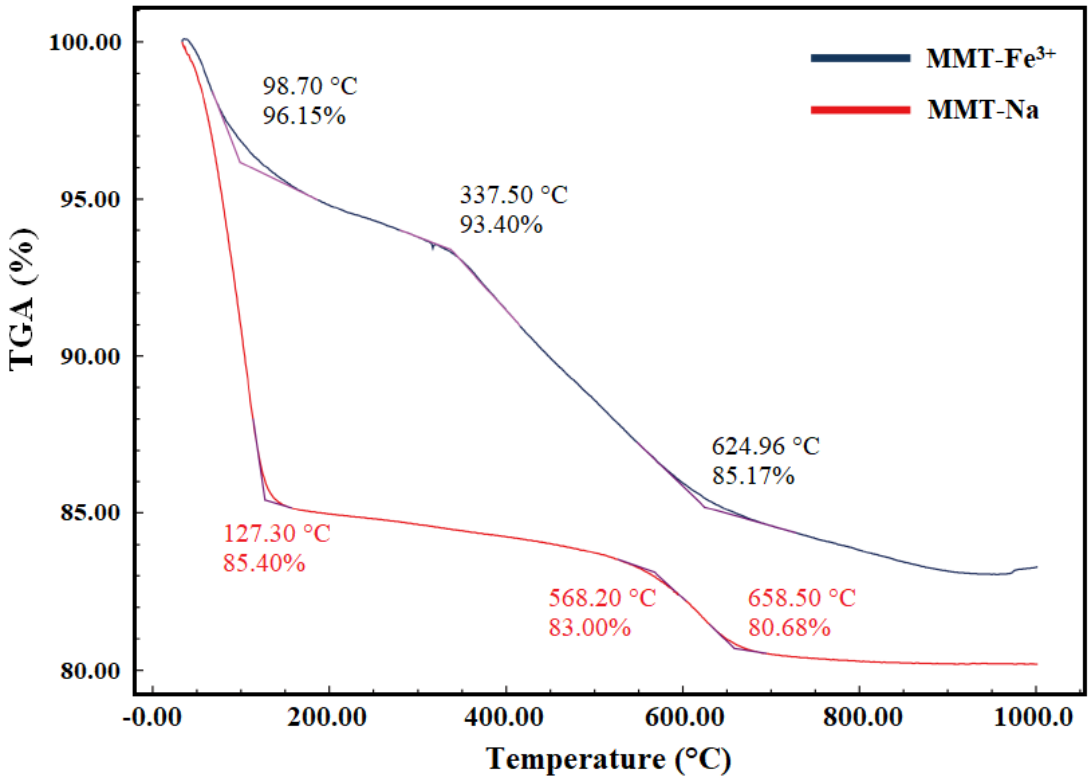

Fig. 4 – TGA of MMT-Na and MMT-Fe^{3+}.

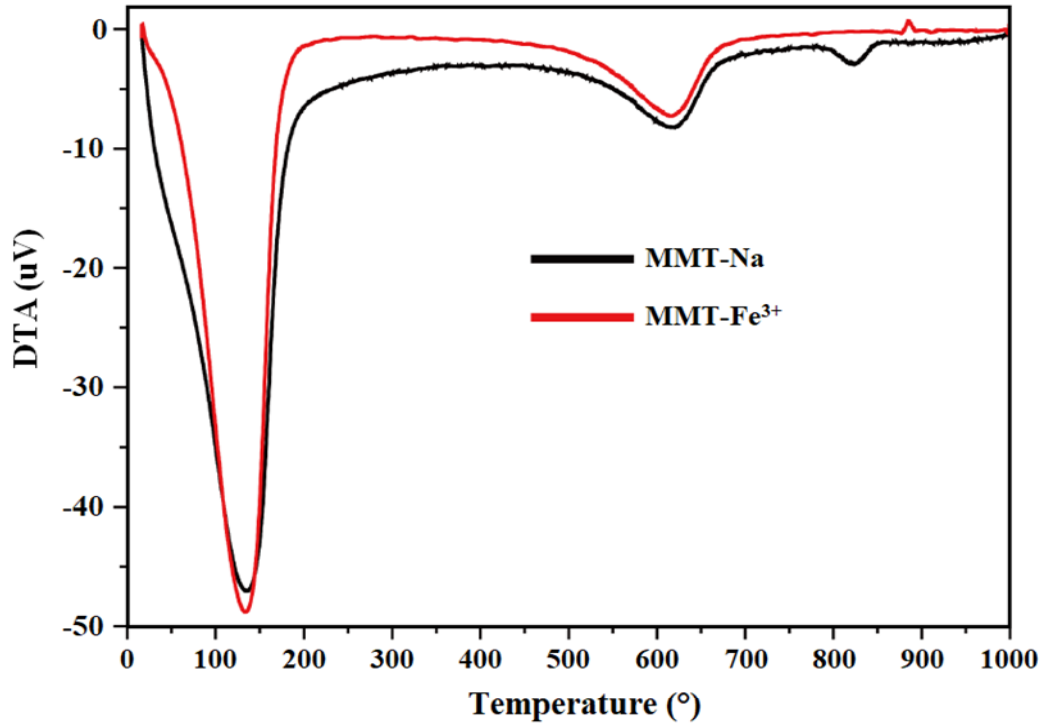

Fig. 5 – DTA of MMT-Na and MMT-Fe^{3+}.

2. CV removal studies

2.1. Effect of adsorbent amount

In order to determine the stoichiometric amount of MMT-Fe^{3+}, it was added to CV dye solution (CV solution 0.025 mM, pH 7) by varying the amount of MMT-Fe^{3+} from 0.01to 0.03 g. The concentration of CV dye removal was estimated from its optical density at λmax = 590 nm using UV–Vis spectrophotometer. The effect of amount MMT-Fe^{3+} on the rate of adsorption of CV solution is depicted in Figure 6. From the Figure 6, it was observed that the required amount of MMT-Fe^{3+} for 100% dye removal was 0.03 g. It was observed that the rate increases with increase in MMT-Fe^{3+} from 0.01 to 0.03 g.

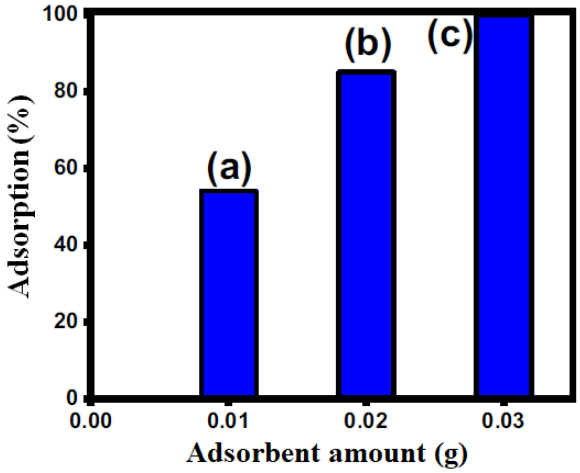

Fig. 6 – Effect of amount MMT-Fe^{3+} on the adsorption of CV (0.025 mM).

2.2. Effect of pH and contact time on CV dye removal

Fig. 7 shows the % removal of CV dye at different pH as a function of time for different solid-to-liquid ratio viz., **a)** MMT-Fe^{3+} is stoichiometrically less (0.01 g, 0.025 mM), **b)** MMT-Fe^{3+} and CV dye are in stoichiometric amounts (0.03 g, 0.025 mM) and **c)** MMT-Fe^{3+} is stoichiometrically excess (0.05 g, 0.025 mM). In general, the dye removal by MMT-Fe^{3+} is very rapid process. In each case, we saw a two-stage removal of CV dye by MMT-Fe^{3+}: a rapid first stage followed by a slow second stage. A complete removal occurred in about 10 min at pH 3 whereas at pH 7 and 10 about 93% removal within 5 min and thereafter 100% reduction occurred within 7 min when stoichiometric amount of MMT-Fe^{3+} was present. From the literature, it was reported that the dye adsorption in acidic solution takes more time when compare to basic solution.[39]

As shown in Fig.7a, when stoichiometrically less amount of MMT-Fe^{3+} (0.01 g, 0.025 mM) was added, we observed a slow reduction around 35–40% removal at pH 3 and pH 7 at 10 min. Reduction was faster and there after the removal efficiency gradually increased from 35 to 60% at pH 3 and 40–75% at pH 7 within 45 min. In both the cases (pH 3 and 7) complete removal was not attained due to the insufficient amount of MMT-Fe^{3+}.

It is well-known that the pH has a significant effect on the adsorption of dye. For instance, Liu *et al.*[40] have demonstrated the application of Cellulose-based Bioadsorbentwith high surface areas for the adsorption and desorption of methylene blue (MB) dye. However the sorption capacity was high at basic pH when compare to acidic pH. A similar observation was made by Ghorai *et al.*[41] for the removal of methylene blue MB and methyl violet (MV) dyes from aqueous solution using a nanocomposite of hydrolyzed polyacrylamide grafted xanthan gum and incorporated nanosilica.

Although these heterogeneous reductants/ adsorbents are used for degradation and adsorption process, there will be an incomplete reduction and time consumption is more. These are effective only in the presence of co-catalysts and sunlight irradiation. However, in the present study we see the efficient removal of CV dye solution both in acidic as well as basic pH.

2.3. Effect of temperature on removal of CV

The reduction of CV dye by MMT-Fe^{3+} was carried out in different temperatures (0–40 °C) at pH 7 in Figure 8. In general, the % dye removal increased with temperature up to 40 °C. The time taken for complete reduction at 0, 30 and 40 °C are 10, 7 and 5 min respectively. Moreover when there was an excess of amount of MMT-Fe^{3+} (Fig. 8c), it took just 5 min, 3 min for the complete reduction of CV at 0 and 30 °C respectively. However, when MMT-Fe^{3+} (Fig. 8a) was stoichiometrically less, the CV dye reduction was only 45 and 52% at 30 and 0 °C even after 1 h. In both the cases complete adsorption is not attained due to the insufficient amount of MMT-Fe^{3+}.

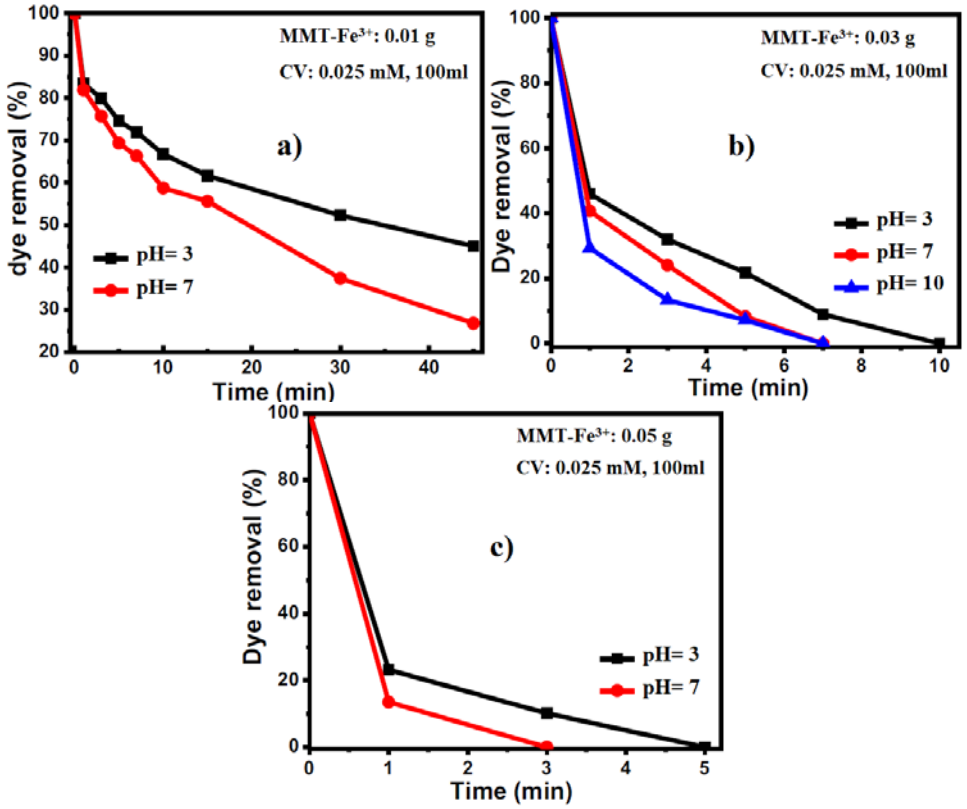

Fig. 7 – Removal of CV dye by: a) Sub-stoichiometric amount of MMT-Fe^{3+} at pH 3 and 7, b) stoichiometric amount of MMT-Fe^{3+} at different pH and c) Excess amount of MMT-Fe^{3+} at pH= 3, 7.

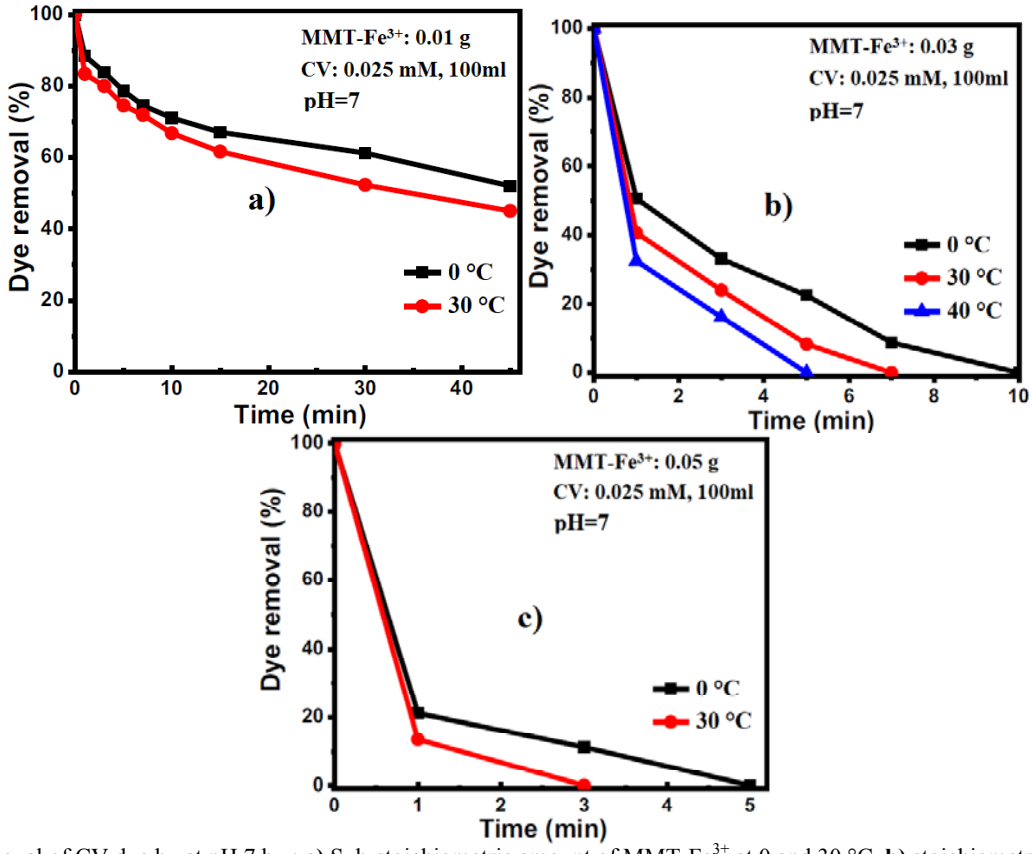

Fig. 8 – Removal of CV dye by at pH 7 by : **a)** Sub-stoichiometric amount of MMT-Fe^{3+} at 0 and 30 °C. **b)** stoichiometric amount of MMT-Fe^{3+} at different temperature. **c)** Excess amount of MMT-Fe^{3+} at 0 and 30 °C.

Chitosan/Fe-hydroxyapatite nanocomposite beads are used for removal of lead (II) ions and CV dye from aqueous solution. The results indicate that increasing the temperature leads to an increase in the adsorption of both metal and dyes.[41] The usage of carbon nanotubes for the adsorption of CV dye from aqueous solution was investigated by Yao et al.[42]. The experimental results have shown that the adsorption capacity increased with increasing temperature (273–333 K), but the removal of CV dye through adsorption on CNTs was found to be rapid at the initial period and then it became slow and stagnate with the increase in contact time. However, in the present study, we see the 100% removal of CV dye from MMT-Fe^{3+} in all the temperatures ranging from 0 to 50 °C.

2.4. Removal Kinetics

Rapid adsorption of CV dye was observed at λmax = 590 nm. From the UV–Vis spectra it was observed that the absorbance of CV dye solution decreases with increasing time intervals which indicates that the dye is degraded rapidly due to the effect of MMT-Fe^{3+}. From the Figure 9, it was obtained that plot of 2+ log O.D. with time was linear and CV dye removal from MMT-Fe^{3+} follows the pseudo first order kinetics. The rate constant was determined using following expression k = 2.303 X Slope. By using this expression rate constant can be easily calculated.

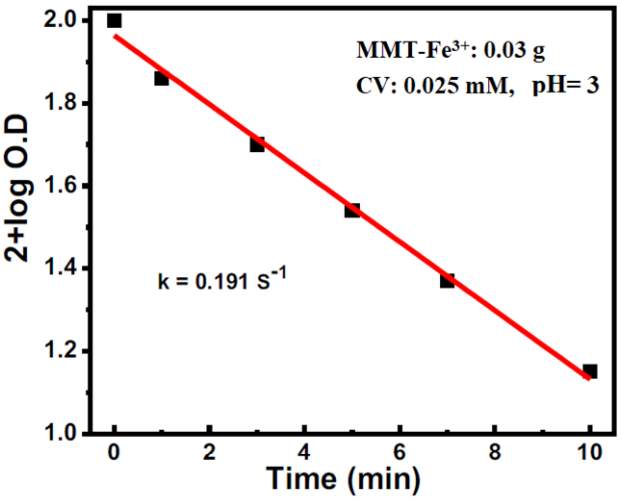

Fig. 9 – Rapid removal of CV dye from MMT-Fe^{3+} follows the pseudo first order reaction.

Wang *et al.*[43] reported the degradation of CV dye by ferrocene via heterogeneous fenton reaction. The experimental results indicated that the degradation of CV dye was found to follow the pseudo first order kinetics. Similarly, Ni/Ti layered double hydroxide is used as a photocatalyst for degradation of aqueous CV dye under visible light condition. The catalytic activity was found to be good under visible light condition and degradation reaction follows pseudo first order kinetics.[44]

2.5. Examination of spent MMT-Fe^{3+}

In order to understand the removal and immobilization CV dye on the MMT-Fe^{3+} nanoclay mineral, it is important to examine the spent or oxidized MMT-Fe^{3+}. As revealed by Fourier transform infrared (FT-IR) spectra Figure 3, the spent clay mineral is intact in all aspects when compared to pure MMT-Fe^{3+}. Also, there is no indication about the presence of additional Fe-dye phase probably due to their small fraction. From the X-ray diffraction (XRD) analysis, we couldn't observe any significant peak in the spent MMT-Fe^{3+} nanoclay mineral. Moreover, in spent MMT-Fe^{3+}, basal spacing d_{001} value was almost the same due to small amount of CV dye adsorbed on the surface and it didn't show a significant peak from XRD analysis.

Figures 10 and 11 represents the morphological images of MMT-Fe^{3+} before and after treating with CV dye solution. In order to understand the reduction and it's adsorption on the clay mineral, it is important to examine the spent or oxidized MMT-Fe^{3+} for Field emission scanning electron microscope with energy dispersive X-ray (SEM/EDXA) analysis. Accordingly, the MMT-Fe^{3+} was analyzed by SEM/EDX spectra to observe any morphological changes upon dye adsorption. In Fig. 11 shows an appreciable change in the microstructure of MMT-Fe^{3+}. Moreover Energy dispersive X-ray (EDXA) analysis confirmed the adsorption of CV dye on the surface of spent MMT-Fe^{3+} as shown in Figure 11.

2.6. Separation of spent MMT-Fe^{3+} from degraded CV solution

After the dye adsorption, the spent MMT-Fe^{3+} settled down at the bottom within 15 min. Then the dispersed spent MMT-Fe^{3+} was removed using centrifugation process. MMT-Fe^{3+} was completely recovered (100%) from degraded CV dye solution. At the end, we got a clear solution which is free from spent MMT-Fe^{3+} clay mineral.

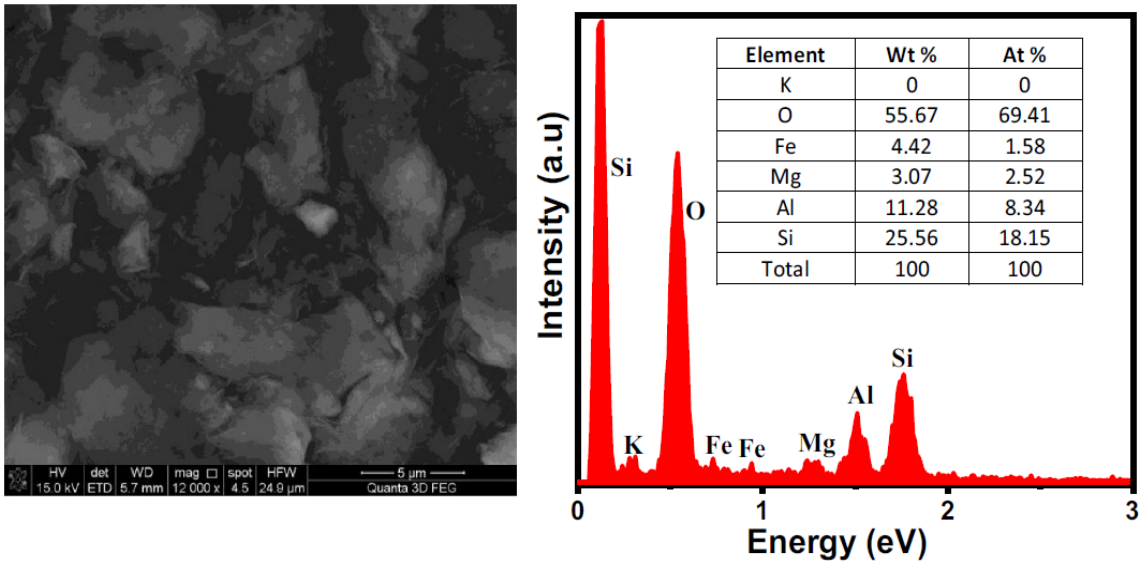

Fig. 10 – FE–SEM with EDX of fresh MMT-Fe^{3+}.

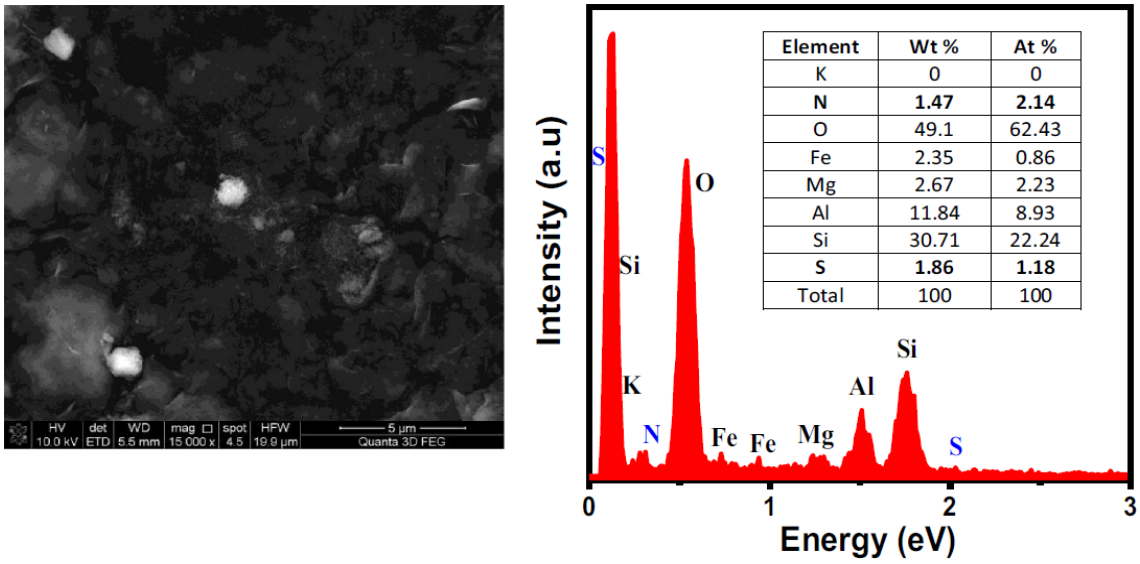

Fig. 11 – FE–SEM with EDX of spent MMT-Fe^{3+}.

The major disadvantage of physical methods is that the dye molecules will be transferred to another phase rather than destroyed. Additionally, biological degradation of organic contaminants suffers from low degradation efficiency, high cost and rigorous degradation conditions. Furthermore, the disposal of chemicals containing sludge at the end of degradation also entails complicated post treatment processes.[45] Graphite powder and carbon nanotubes have been used for the removal of organic dyes from aqueous wastewater; however these adsorbents usually suffer from difficulties in the separation and regeneration processes. Furthermore activated carbon was used in the removal of dyes and pigments, but the main disadvantage is activated carbon regeneration which typically involves drying at elevated temperature.[46] Therefore, it is indispensable and emergent to explore the new reductant/adsorbent for the dye removal which could be completely separated from the degraded solution easily. Accordingly, we have successfully achieved the complete (100%) separation of spent MMT-Fe^{3+} from the degraded CV dye solution by centrifugation. From the experimental results, it was shown that the separation of MMT-Fe^{3+} from aqueous solution could be efficient, facile and reliable. Nevertheless, MMT-Fe^{3+} was a suitable reductant for the adsorption of dye molecules from aqueous solution with high efficiency, low cost and environmental friendliness.

2.7. Comparison with other adsorbents/reductants

Zhang *et al*. has described the application of porous Co_3O_4 nanorods-reduced graphene (PCNG) oxide hybrid materials for the catalytic oxidation of CV dye. PCNG showed 97% degradation after 25 min in the presence of H_2O_2. However there was no degradation without PCNG or H_2O_2.[47] Furthermore, Fe doped ZnS nanoparticles[48] and ferrite bismuth nanoparticles[49] exhibited good photocatalytic activity of CV dye but only under visible light irradiation. $CoFe_2O_4$/activated carbon nanocomposites have shown 99% CV adsorption in 50 min.[50] Au-tipped CdSe nanorod clusters are also used as photo catalysts for CV reduction via multiple electron reduction under aerobic conditions.[51] The main drawbacks of afore mentioned are: the reductants/adsorbents have shown incomplete reduction, time consumption is more, effectiveness only in presence of co-catalyst or additives and rapid reduction was only under visible light irradiation conditions.

Hence metal nanoparticles have considerably faded its importance for dye degradation processes.[52] Hence it is essential to propose a suitable material which acts both as reductant and adsorbent for field applications, especially to treat water and soil. We believe that MMT-Fe^{3+} could be the efficient, facile and reliable reductant/adsorbent for the remediation of dyes from aqueous solution.

CONCLUSIONS

In this work, we have reported MMT-Fe^{3+} as an effective reductant cum adsorbent for removal of CV dye solution from aqueous solution through adsorption process under ambient conditions. The removal of CV dye from aqueous solution can be achieved rapidly through adsorption process by MMT-Fe^{3+} at solid–liquid ratio, different pH and temperature. The decrease in CV dye concentration due to reaction between MMT-Fe^{3+} was expressed here in terms of % reduction as a function of time. In general the dye removal by MMT-Fe^{3+} is a rapid process, especially under stoichiometric conditions. The CV removal was rapid at basic pH and increases with temperature up to 40 °C. A complete reduction (100%) occurred in about 7 min at pH 7 and 10, while at pH 3, in about 10 min. The time taken for complete reduction at 0, 30 and 40 °C are 10, 7 and 5 min respectively. The experimental results of CV dye removal from MMT-Fe^{3+} followed the pseudo first order kinetics. The adsorption of the degraded CV dye on spent clay mineral was confirmed from SEM/ EDAX analysis. More importantly, MMT-Fe^{3+} could be separated and retrieved easily after the reaction by centrifugation from the degraded CV dye solution. The enhanced removal efficiency makes MMT-Fe^{3+} clay mineral a promising adsorbent/reductant for environmental remediation of cationic pollutants and could be applied in the purification of drinking water and large scale of industrial wastewater.

REFERENCES

1. E. Zelić, Ž. Vuković and I. Halkijević, *GRAĐEVINAR*, **2018**, *70*, 315-323.
2. Y. Tzvi and Y. Paz, *J. Photochem. Photobio. A: Chem.*, **2019**, *372*, 63–70.
3. C. Berberidou, V. Kitsiou, D. A. Lambropoulou, A. Antoniadis and E. Ntonou, *J. Environ. Manage*. **2017,** *195* 133–139.
4. I. Carra, J. A. S. Pérez, S. Malato, O. Autin and B. Jefferson, *Chem. Eng. J*., **2015**, *264*, 690–696.
5. D. Adak, B. Show, A. Mondal and N. Mukherjee, *J. Catal.* **2017**, *355*, 63–72.
6. A. Mittal, J. Mittal, A. Malviya, D. Kaur and V.K. Gupta, *J. Colloid Interface Sci*., **2010**, *343*, 463–473.
7. S. Neupane, S. T. Ramesh, R. Gandhimathi and P. V. Nidheesh, *Desal. Water Treat*., **2015**, *54*, 2041–2054.
8. L. B. L. Lim, N. Priyantha, T. Zehra, C. W. Then and C. M. Chan, *Desal. Water Treat*., **2016**, *57,* 10246–10260.
9. R. Sivashankar, A. B. Sathya, K. Vasantharaj and V. Sivasubramanian, *Environ. Nanotechnol. Monit. Manage*., **2014**, *1–2*, 36–49.
10. N. Askari, M. Farhadian, A. Razmjou and H. Hashtroodi, *Desalin. Water Treatment*, **2016**, *57*, 18194-18201.
11. S. Demieregea, A. Toptasb, E. Mavioglu Ayanb, I. Yasac and J. Yanik, *Chem. Ecology*, **2015**, *31,* 1-14.
12. J. Huang and H. Zhang, *Environ. Int.*, **2019**, *133*, 105141.
13. F. Ghanbari and M. Moradi, *Chem. Eng. J.*, **2017**, *310*, 41–62.
14. W. D. Oh, Z. Dong and T. T. Lima, *Appl. Cat. B: Environ.*, **2016,** *194*, 169–201.
15. T. Y. Mustafa, K. S. Tushar, A. Sharmeen and H. M. Ang, *Adv. Coll. Interface Sci*., **2014**, *209*, 172–184.
16. V. O. Njoku, K. Y. Foo, M. Asif and B. H. Hameed, *Chem. Eng. J.* **2014**, *250*, 198–204.
17. M. Horta, M. Aguilar, F. Moura, J. Campos, V. Ramos, and A. Quizunda, *Mater. Today: Proceed.*, **2019**, *14*, 716–721.
18. P. Zhiguo, Y. Shuang, L. Lingyun, L. Chunmei, Z. Shuzhen and G. Baoyuan, *Environ. Pollut.,* **2014**, *184*, 579–585.
19. S. Gu, X. Kang, L. Wang, E. Lichtfouse and C. Wang, *Environ. Chem. Lett*., **2019,** *17*, 629-654.

20. L. S. Kostenko, I. I. Tomashchuk, T. V.Kovalchuk and O. A. Zaporozhets, *Appl. Clay Sci*., **2019**, *172*, 49–56.
21. A. A. Adeyemo, I. O. Adeoye and O. S. Bello, *Appl. Water Sci.*, **2017**, *7*, 543–568.
22. M. D. Castro, L. B. Abad, D. G. Sumalinog and R. R. Abarca, *Sustainable Environ. Res.*, **2018**, *28*, 197-205.
23. Y. S. Ngoh and M. A. Nawi, *Int. J. Environ. Sci. Technol.*, **2016**, *13*, 907–926.
24. M. K. Uddin, *Res. J. Chem. Environ*., **2017,** *308*, 438–462.
25. S. A. Hamid, M. Shahadat and S. Ismail, *Appl. Clay Sci*., **2017,** *149*, 79–86.
26. J. N. Putro, S. P. Santoso, S. Ismadji and Y. H. Ju. *Microporous Mesoporous Mater*., **2017**, *246*, 166–177.
27. T. Ngulube, J. R. Gumbo, V. Masindi and A. Maity, *J. Environ. Manag*., **2017**, *191*, 35–57.
28. T. Grygar, D. Hradil, P. Bezdicka, B. Dousova, L. Capek and O. Schneeweiss. *Clays and Clay Minerals,* **2007**, *2,* 165–176.
29. C. Leungo, V. Puccia and M. Avena, *J. Hazardous Mater.,* **2010,** *2,* 1713–1719.
30. B. M. Vinoda and J. Manjanna, *Appl. Clay Sci.,* **2014,** *97,* 78–83.
31. R. Fabryanty, C. Valencia, F. Edi Soetaredjo and S. Ismadji, *J. Environ. Chem. Eng*., **2017,** *5,* 5677–5687.
32. L. N. Shi, X. Zhang and Z. L. Chen, *Water Research,* **2011**, *45,* 886–892.
33. K. Jlassi, R. Abidi, M. Benna, M. M. Chehimi, P. Kasak and I. Krupa, *Appl. Clay Sci*., **2018**, *161*, 15–22.
34. S. Boudjemaa, *Rev. Roum. Chim.,* **2019**, *64*, 35-44.
35. M. F. Brigatti, C. Lugli, G. Cibin and A. Marcelli, *Clays and Clay Minerals*, **2000,** *48,* 272–281.
36. J. Manjanna, T. Kozaki, N. Kozai and S. Sato, *J. Nuclear Sci. Techn.,* **2007**, *44,* 929–932.
37. N. Kozai, Y. Adachi, S. Kawamura, K. Inada, T. Kozai and S. Sato, *J. Nuclear Sci. Techn.,* **2001**, *38,* 1141-1143.
38. D. L. Guerra, V. P. Lemos, C. Airoldi and R. S. Angélica, *Polyhedron*, **2006,** *25*, 2880-2890.
39. S. Sohrabnezhad, A. H. Yangjeh and S. Eftekhari, *Int. J. Nano Dimens*. **2013,** *4*, 91-104.
40. L. liu, Z. Y. Gao and X. P. Su, *A.C.S. Sustainable Chem. Eng.* **2015**, *3*, 432–442.
41. S. Ghorai, A. Sarkar, M. Raoufi, B. A. Panda, H. Schoonherr and S. Pal, *A.C.S. Appl. Mater. Interfaces,* **2014,** *6,* 4766–4777.
41. S. S. Samaneh, S. Saeed, N. Nezafati and K. Yahya, *J. Environ. Management***, 2014**, *146,* 481–490.
42. Y. Yao, F. Xu, M. Chen, Z. Xu and Z. Zhu, *Bioresource Technology,* **2010**, *101,* 3040–3046.
43. Q. Wang, S. Tian and P. Ning, *Ind. Eng. Chem. Res.,* **2014,** *53,* 643–649.
44. P. R. Chowdhury and K. G. Bhattacharyya, *Dalton Transactions*, **2015**, *44*, 6809-6824.
45. Z. Mao, Q. Wu, M. Wang, Y. Yang, J. Long and X. Chen, *Nanoscale Res. Lett.,* **2014**, *9,* 501.
46. X. He, K. B. Male, P. N. Nesterenko, D. Brabazon, B. Paull and J. H. T. Luong, *Appl. Mater. Interfaces,* **2013**, *5,* 8796–8804.
47. Z. Zhang, J. Hao, W. Yang, B. Lu, X. Ke and B. Zhang, *A.C.S. Appl. Mater. Interfaces*, **2013**, *5*, 3809–3815.
48. R. Chauhan, A. Kumar and R. P. Chaudhary, *Spectrochim. Acta Part A Molec. Biomolec. Spectroscopy,* **2013**, *113,* 250–256.
49. T. Soltani and M. H. Entezari, *J. Molec. Catal. A Chem.,* **2013**, *377,* 197–203.
50. M. R. Heidari, R. S. Varma, M. Ahmadian and M. Pourkhosravant, *Appl. Sci*. **2019**, *9*, 963.
51. Z. Li, Y. Hu and Y. Sun, *Chem. Comm.,* **2014***, 50,* 1411–1413.
52. M. Vinothkannan, C. Karthikeyan, G. G. Kumar and A. R. Kim, *Spectrochim. Acta Part A Molec. Biomolec. Spectroscopy,* **2015**, *136,* 256–264.